

See discussions, stats, and author profiles for this publication at: <https://www.researchgate.net/publication/235894009>

Probing Stereoelectronic Interactions in an O–N–O Unit by the Atomic Energies: Experimental and Theoretical Electron Density Study

ARTICLE *in* THE JOURNAL OF PHYSICAL CHEMISTRY A · MARCH 2013

Impact Factor: 2.69 · DOI: 10.1021/jp312835y · Source: PubMed

CITATIONS

4

READS

22

2 AUTHORS, INCLUDING:



[Konstantin A Lyssenko](#)

Russian Academy of Sciences

761 PUBLICATIONS 6,115 CITATIONS

SEE PROFILE

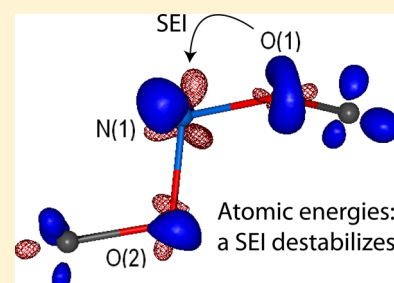
Probing Stereoelectronic Interactions in an O–N–O Unit by the Atomic Energies: Experimental and Theoretical Electron Density Study

Yulia V. Nelyubina* and Konstantin A. Lyssenko

A.N. Nesmeyanov Institute of Organoelement Compounds of Russian Academy of Sciences, 119991, Vavilova Str., 28, Moscow, Russia

S Supporting Information

ABSTRACT: Stereoelectronic interaction $\text{lp}(\text{O}1) \rightarrow \sigma^*(\text{N}1-\text{O}2)$ in a O–N–O unit was analyzed by means of R. Bader's Atoms in Molecule theory on the basis of X-ray diffraction data for dimethyl-(2*R*,4*aR*,5*S*,7*R*)-2,5,7-triphenylhexahydro-4*H*-[1,2]oxazino[2,3-*b*][1,2]oxazine-4,4-dicarboxylate. Atomic energies obtained by applying this approach to both the experimental and theoretical electron densities were used to probe the energy of this strong stereoelectronic interaction, giving consistent results with the NBO analysis, although showing its destabilizing character.



INTRODUCTION

One of the key concepts in organic stereochemistry is the anomeric effect.^{1,2} Introduced to explain the stabilization of six-membered carbohydrate rings with an electronegative substituent at the C1 position in biological molecules, it rationalizes the conformational preferences of many organic compounds. If they contain the R–X–C–Y atomic arrangement with X bearing at least one lone electron pair (lp) and Y being an electronegative atom, they tend to adopt *gauche* conformation; such a behavior is known as the generalized anomeric effect.^{1,2}

The most accepted explanation for this phenomenon involves the so-called hyperconjugative model as the special case of the stereoelectronic model, attributing it to the electron transfer from a lone pair of the atom X to the antibonding orbital C–Y that is favored by the antiperiplanar configuration of the moiety lp–X–C–Y.^{1,2} Such a description of the anomeric effect was proposed on the basis of natural bond orbital (NBO) analysis³ showing the largest individual contribution in the stabilization of a system in a *gauche* conformation to come from the above charge transfer $\text{lp}(\text{X}) \rightarrow \sigma^*(\text{C}-\text{Y})$. Further NBO studies,^{4–7} however, demonstrated that other contributions (stereoelectronic interactions involving nonpolar bonds and steric and electrostatic effects) should be taken into account.

Another interpretation of the anomeric effect has been given recently^{8–10} with the help from R. Bader's Atoms in Molecule (AIM) theory.¹¹ The latter not only allows dealing with atomic parameters such as charge and energy¹² (and so describing the anomeric effect in these terms^{8–10}) but also helps identifying all the interatomic interactions in a system (and so analyzing the influence of the environment on it^{13,14}).

Within the AIM approach, another interpretation of the anomeric effect using atomic charges and energies (obtained by

integrating electron density and electronic energy density over atomic basins¹¹) was provided for OCO ^{8,9} and NCN ^{10,13} as well as NCS ¹³ systems. It implies the key role of central hydrogen atoms (those of the CH_2 or CHR groups), which experience the outflow of the electron density to the other atoms of the unit X–C–Y accompanying the anomeric stabilization of the system. This trend is not in line with the classic hyperconjugative model suggesting the dominance of the $\text{lp}(\text{X}) \rightarrow \sigma^*(\text{C}-\text{Y})$ contribution. However, an lp–X–C–Y stereoelectronic interaction was shown to cause the loss of charge (and energy) by the atom X and gain of it by the atom Y,¹³ as can be expected from this model. The central hydrogen atoms, however, interfere with this charge flow process, so the atom Y acquires more charge density than is lost by X, and most of it comes from those hydrogens. So the question arises how the charge and energy transfer resulted from a stereoelectronic interaction (SEI) in a system with no central hydrogen atoms complies with two different descriptions of the anomeric effect, those based on the NBO analysis and AIM atomic charges and energies.

To check how both of them, one supporting the hyperconjugative model but giving some sort of a measure for strength of an individual SEI and the other being more physically sound but including all contributions from all SEIs in a molecule, will perform in such a case, we used dimethyl-(rel-2*S*,4*aS*,5*R*,7*R*)-2,5,7-triphenylhexahydro-4*H*-[1,2]oxazino[2,3-*b*][1,2]oxazine-4,4-dicarboxylate (**1**, Figure 1). Its molecular geometry is strongly suggestive of the SEI lp–O(1)–N(1)–O(2) in its O–N–O unit, which has not been thoroughly

Received: December 29, 2012

Revised: March 6, 2013

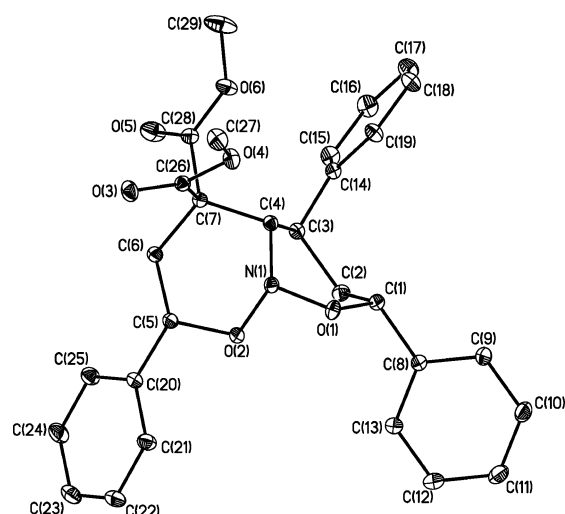


Figure 1. General view of a molecule **1** in representation of atoms via thermal ellipsoids at 50% probability level (the hydrogen atoms are not shown).

analyzed in this respect before. With no interference from central hydrogen atoms (as they are absent here) but with other SEIs expected from the geometrical considerations (see below), it makes the perfect fit for putting the two methods for quantifying SEI to test.

For this purpose, we performed the NBO study and AIM-based topological analysis of the electron density distribution obtained theoretically (by quantum chemistry) for **1**, its sister isomer without that SEI, to make possible analyzing its role in a stabilization of the molecular conformation of **1**, and their

unsubstituted analogues (see Scheme 1) as well as experimentally (by high-resolution X-ray diffraction) for **1**. The latter, made possible by the availability of high quality crystals of **1**, also tempted us to try using the difference in the atomic energy of the two oxygen atoms involved in the SEI in O–N–O unit for the quantitative estimation of the strength of a SEI from the experimental data only.

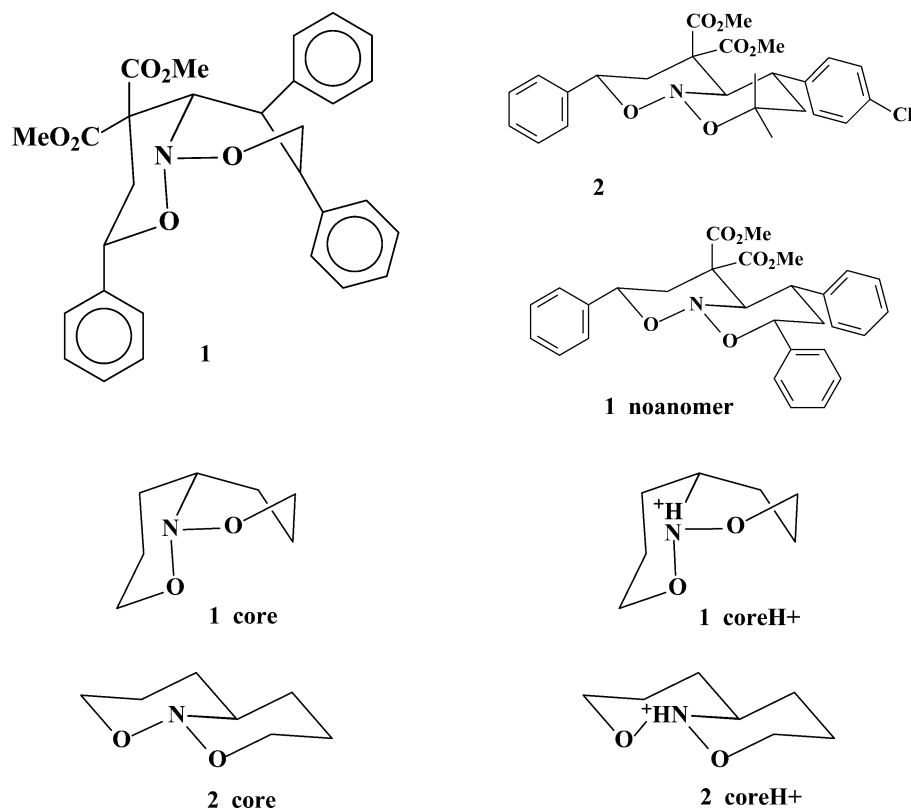
The presence of the second independent molecule of **1** in an asymmetric unit ($Z' = 2$) is an extra advantage that allows additionally judging the validity of the trends observed in the experimental atomic charges and energies. Those can also be used to examine the pseudosymmetry phenomenon at the atomic energy level; this has been already done for the atomic charges and interaction energies.^{15,16}

■ EXPERIMENTAL SECTION AND COMPUTATIONAL DETAILS

The systems analyzed in this study will be referred to in the text as shown in Scheme 1.

High-resolution X-ray diffraction experiment was performed for a single-crystal of the compound **1** ($C_{29}H_{29}NO_6$, $M = 487.53$) obtained from its dichloromethane solution. The crystals are triclinic, space group $P\bar{1}$, at 100 K: $a = 11.3043(2)$, $b = 13.5609(2)$, $c = 16.6403(3)$ Å, $\alpha = 78.6600(10)$, $\beta = 73.5170(10)$, $\gamma = 86.7910(10)^\circ$, $V = 2398.32(7)$ Å³, $Z = 4$ ($Z' = 2$), $d_{\text{calc}} = 1.350$ g cm⁻³, $\mu(\text{MoK}\alpha) = 0.94$ cm⁻¹, $F(000) = 1032$. Intensities of 478 533 reflections were measured with a Bruker APEX II DUO CCD diffractometer [$\lambda(\text{MoK}\alpha) = 0.71072$ Å, ω -scans, $2\theta < 110^\circ$], and 60 670 independent reflections [$R_{\text{int}} = 0.0617$] were used in further refinement. The structure was solved by the direct method and refined by the full-matrix least-squares technique against F^2 in the anisotropic–isotropic

Scheme 1. Schematic Representation of the Systems Analyzed, Illustrating the Conformation of the Heterocyclic Core



approximation. Hydrogen atoms were located from the Fourier synthesis of the electron density and refined in the isotropic approximation. The refinement converged to $wR_2 = 0.1535$ and $GOF = 1.003$ for all the independent reflections ($R_1 = 0.0464$ was calculated against F for 41 156 observed reflections with $I > 2\sigma(I)$). All calculations were performed using SHELXTL PLUS 5.0.¹⁷ CCDC 917300 contains the supplementary crystallographic information for **1**; the data for its sister compound **2** that we have also X-rayed (see Supporting Information) are available as CCDC 912763.

The multipole refinement of the experimental data for **1** was carried out within the Hansen–Coppens formalism¹⁸ using XD program package¹⁹ with the core and valence electron density derived from wave functions fitted to a relativistic Dirac–Fock²⁰ solution. Before the refinement, the C–H bond distances were normalized to the standard value of 1.08 Å. The level of multipole expansion was octupole for non-hydrogen atoms, and the dipole D_{10} were refined for hydrogen atoms. The refinement was carried out against F and converged to $R = 0.0262$, $R_w = 0.0243$ and $GOF = 0.89$ for 30 425 merged reflections with $I > 3\sigma(I)$. All bonded pairs of atoms satisfy the Hirshfeld rigid-bond criteria²¹ (difference of the mean square displacement amplitudes along the bonds was not larger than 9×10^{-4} Å²). The potential energy density $v(\mathbf{r})$ was evaluated through the Kirzhnits’ approximation²² for the kinetic energy density function $g(\mathbf{r})$. Accordingly, the $g(\mathbf{r})$ function is described as $(3/10)(3\pi^2)^{2/3}[\rho(\mathbf{r})]^{5/3} + (1/72)|\nabla\rho(\mathbf{r})|^2/\rho(\mathbf{r}) + 1/6\nabla^2\rho(\mathbf{r})$, what in conjunction with the local virial theorem ($2g(\mathbf{r}) + v(\mathbf{r}) = 1/4\nabla^2\rho(\mathbf{r})$) leads to the expression for $v(\mathbf{r})$ and makes possible to estimate the electron energy density $h_e(\mathbf{r})$. The total electron density function was positive everywhere, and the maxima of the residual electron density located in the vicinity of nuclei (the largest being near the atom O(1A)) were not more than 0.2 e Å⁻³. Analysis of topology of the $\rho(\mathbf{r})$ function was carried out using the WINXPRO program package.²³ The integration over atomic basins was performed numerically, leading to the charge leakage of less than 0.02 e. The sum of the atomic volumes of the two independent molecules of **1** in a crystal (1193.39 Å³) reproduced well the volume of an independent part of the unit cell (1199.16 Å³) with relative error 0.5%. Although the integrated Langrangian ($L(\mathbf{r}) = -1/4\nabla^2\rho(\mathbf{r})$) for every atomic basin has to be exactly zero, a reasonably small value averaging to 0.06×10^{-4} au was obtained.

The interaction energies from X-ray diffraction data for **1** were estimated via the Espinosa’s correlation, a semi-quantitative relationship between the energy of an interaction and the value of the potential energy density function $v(\mathbf{r})$ in the CP(3,–1).^{24,25} This approach gives very accurate estimates in many cases: weak interactions such as H⋯H²⁶ and C–H⋯O,²⁷ strong and intermediate hydrogen bonds,^{28,29} etc.

The DFT calculations of the isolated molecule **1** and its sister isomer **1_noanomer** and those of their model unsubstituted analogues (Scheme 1), both in molecular (**1_core** and **2_core**) and in protonated (**1_coreH+** and **2_coreH+**) forms, were performed with the Gaussian09 program package³⁰ using the B3LYP functional. Full optimization of their geometry was carried out with the 6-311G(d,p) basis set starting from the X-ray structural data. The extremely tight threshold limits of 2×10^{-6} and 6×10^{-6} au were applied for the maximum force and displacement, respectively. During the optimization, the type of a saddle point on the potential energy surface (PES) was determined by force constant matrix calculations. All obtained

geometries corresponded to a global minimum on PES. The topological analysis of the computed electron densities was performed using AIMall program package.³¹ The difference in molecular virial ratio was as low as 1.91×10^{-5} .

RESULTS AND DISCUSSION

Molecular and Crystal Geometry from X-ray Diffraction Data. According to the X-ray diffraction data (XRD), the compound **1** crystallizes with two independent species in an asymmetric part of the unit cell having the same molecular geometry (Figure S1 of Supporting Information) with two distinct N–O distances: the short bond N(1)–O(1) (1.3914(5) and 1.3867(5) Å in two independent species) and the long bond N(1)–O(2) (1.4694(5) and 1.4662(5) Å). Such an asymmetry is characteristic for the compounds containing C₁–O–N–O–C₂ moiety: out of 71 ordered structures available in Cambridge Structural Database (CSD, version 5.33³²), only 9 were found with these bond lengths being close (in most of these cases C₁ was identical to C₂); the mean difference between the two N–O bond lengths was 0.05 Å. This difference between the two distances involving the oxygen atoms in a very similar molecular environment (up to 0.08 Å in **1**) agrees with the presence of the SEI lp-O(1)–N(1)–O(2) stabilizing such a distorted geometry. Indeed, one of the oxygen’s lone pairs (both placed theoretically) is in a favorable position for the latter to occur, the pseudotorsion angle lp-O(1)–N(1)–O(2) being 157.7 and 165.1° in the two independent molecules of **1**.

Note that the isomer 2S,4aR,5S of its analogue with two methyl groups instead of a phenyl at the atom C(1) (hereinafter denoted as **2**, its structure is shown in Figure S2 of Supporting Information) have two N–O bonds that are nearly identical (1.4557(15) and 1.4593(15) Å). Both the heterocycles in **2** adopt a chair conformation; the atoms N(1) and C(6) deviate from the plane of the others by 0.83(1) and 0.66(1) Å and the atoms O(1) and C(3) by 0.73(1) and 0.64(1) Å. When going back to the compound **1**, the conformation of the first cycle persists (with the deviation of the same atoms equal to 0.82(1) and 0.65(1) Å), while that of the O(1)-containing ring becomes significantly distorted (Figure 2). In this case, the atoms that deviate the most (by 0.63(1)–0.69(1) Å) are N(1) and C(1).

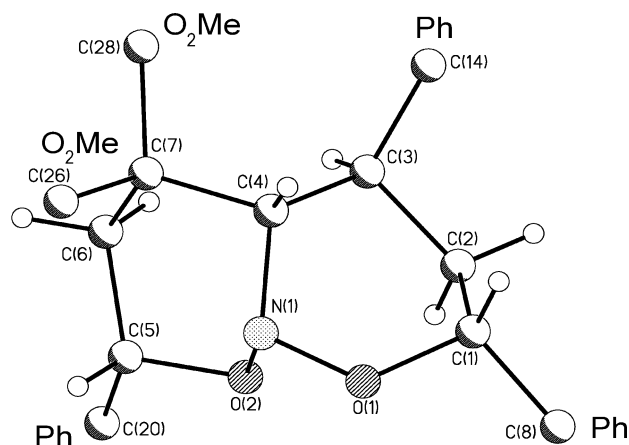


Figure 2. Schematic representation of the heterocyclic core showing the labeling scheme used in further discussion for both the compounds **1** and **2**.

On the basis of the geometrical criteria, other SEIs involving the bonds N–C, C–C, or C–H are expected in both systems; the largest values of the corresponding pseudotorsion angles vary from 129.2 to 175.5° in **1** and from 161.1 to 177.5° in **2**. The latter allow placing lp-N(1)–O(1)–C(1) and lp-N(1)–C(3)–C(4) in **1** or lp-O(2)–C(5)–C(6) and lp-O(1)–C(1)–C(2) in **2** among the strongest SEIs here (see below). Overall, they are, however, not very different between the two compounds, as evidence by the minor differences in the bond lengths other than N–O (see Table 1) not exceeding 0.01 Å.

Table 1. Selected Bond Lengths in **1, Its Analogue **2**, and **1_noanomer** (the Isomer of **1** without the SEI lp-O(1)–N(1)–O(2))**

bond	1		2		1_noanomer
	experiment ^a	theory	experiment	theory	
N(1)–O(1)	1.3914(5) [1.3867(5)]	1.382	1.4557(15)		1.430
N(1)–O(2)	1.4694(5) [1.4662(5)]	1.468	1.4593(15)		1.433
O(1)–C(1)	1.4687(6) [1.4751(6)]	1.473	1.4660(17)		1.429
C(1)–C(2)	1.5207(7) [1.5220(7)]	1.526	1.5341(19)		1.530
C(2)–C(3)	1.5517(6) [1.5546(6)]	1.556	1.549(2)		1.545
C(3)–C(4)	1.5472(6) [1.5516(6)]	1.554	1.564(2)		1.558
N(1)–C(4)	1.4819(5) [1.4757(5)]	1.479	1.5037(17)		1.495
O(2)–C(5)	1.4397(5) [1.4369(6)]	1.442	1.4507(17)		1.431
C(5)–C(6)	1.5242(6) [1.5347(6)]	1.528	1.533(2)		1.534
C(6)–C(7)	1.5383(6) [1.5406(6)]	1.545	1.562(2)		1.558
C(4)–C(7)	1.5552(6) [1.5535(6)]	1.564	1.5891(19)		1.577

^aThe values for the second independent molecule are given in brackets.

Although the latter conclusion can be hindered by rather mediocre quality of the data set for the compound **2**, the main contribution to the stabilization of a distorted conformation in **1** is still expected to come from the SEI lp-O(1)–N(1)–O(2) with the energy of 16.09 kcal/mol according to the NBO data (see below). Note that a new series of related compounds with CCDC 912759, 912760, and 912761 have the same distorted

conformation; that with CCDC 912762 is similar to **2** (their synthesis was recently reported in ref 33).

The crystal packing effects in this case should not affect much of the molecular geometry. In crystal **1**, the molecules form only weak van der Waals interactions. Those are C–H...O, C–H... π , and H...H ones with the lowest interatomic distances being 2.56(1), 2.74(1) and 2.34(1) Å, respectively. The same concerns the compound **2**: the shortest C–H...O and H...H contacts therein are as long as 2.50(1) and 2.27(1) Å. The strongest interaction that may slightly interfere with the characteristics of the anomeric moiety in **1** is an intramolecular C(2)–H(2B)...O(2) contact (O...H 2.38(1) and 2.41(1) Å).

Experimental Electron Density Analysis of **1.** To get more quantitative information on the role of interatomic interactions in the anomeric stabilization, we performed the high-resolution XRD investigation of **1** that gave us the electron density distribution function $\rho(\mathbf{r})$ we then analyzed within the AIM theory.¹¹ Note that the resulting deformation electron density distribution (DED) in the unit ONO confirmed the antiperiplanar disposition of one of the lone pairs at the oxygen atom O(1) in respect to the bond N(1)–O(2); the corresponding electron density accumulation domains were found for both the oxygens (two per each atom) as well as for the atom N(1) bearing one lp (Figure 3A). The electron localization function (ELF) obtained from the experimental data, which is more physically sound and more suitable for this purpose,³⁴ provided the same qualitative picture on the location of lps in the ONO unit as the DED distribution did (Figure 3B).

The following topological analysis of the experimental $\rho(\mathbf{r})$ function performed for **1** revealed the bond critical points (3,–1) or BCPs, which are the unambiguous indicator of a bonding interaction according to AIM,¹¹ for all the above intermolecular interactions and some of those that were impossible to suspect on the basis of the geometrical criteria only. The values of $\rho(\mathbf{r})$ and $\nabla^2\rho(\mathbf{r})$ in these BCPs are extremely low (not more than 0.05 e Å^{–3} and 0.9 e Å^{–5}, respectively) showing that the interactions above are indeed very weak. In particular, their energy estimated by Espinosa's correlation^{24,25} varies from 0.3 to 1.5 kcal/mol in the case of the intermolecular interactions (see Table S2 of Supporting Information). For comparison, the interaction energy value of ~3.5 kcal/mol (see Table S1A of Supporting Information) was observed for the intramolecular C–H...O bond involving the atoms O(2); $\rho(\mathbf{r})$ and $\nabla^2\rho(\mathbf{r})$ in the corresponding BCP are 0.11 e Å^{–3} and 1.6 e Å^{–5}. (Its topological and energetic parameters were reproduced very

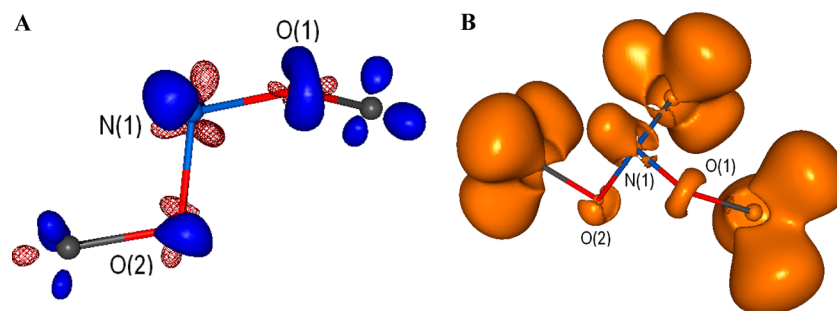


Figure 3. Three-dimensional distributions in the section of the ONO unit in a crystal of **1** (a) of the deformation electron density (isosurface with DED = 0.4 e Å^{–3} is shown by red; negative isosurface with DED = –0.4 e Å^{–3} by wireframe) and (b) of the electron localization function (isosurface with ELF = 0.8). Pseudoatomic contributions of the atoms O(1), N(1), O(2), C(1), C(4), and C(5) were included in the cluster used for the function construction.

Table 2. Atomic Charges and Energies^a for the Core Atoms in **1** and **1_noanomer**

atom	1				1_noanomer	
	experiment ^b		theory		theory	
	charge	energy	charge	energy	charge	energy
N(1)	−0.06 [−0.06]	54.4572 [54.4585]	−0.04	54.7095	−0.05	54.6857
O(1)	−0.60 [−0.59]	75.1760 [75.2173]	−0.64	75.6409	−0.69	75.7090
O(2)	−0.63 [−0.63]	75.2202 [75.2526]	−0.71	75.6915	−0.69	75.7054
C(1)	+0.16 [+0.19]	38.3051 [38.2945]	+0.40	37.8298	+0.47	37.7905
C(2)	−0.29 [−0.25]	38.6635 [38.5560]	+0.04	38.0424	+0.04	38.0510
C(3)	−0.10 [−0.09]	38.4706 [38.4401]	+0.04	38.0111	+0.04	38.0190
C(4)	+0.09 [+0.07]	38.3603 [38.3754]	+0.30	37.9125	+0.28	37.9012
C(5)	+0.21 [+0.23]	38.2600 [38.2593]	+0.45	37.7949	+0.47	37.7932
C(6)	−0.25 [−0.27]	38.5457 [38.6099]	+0.04	38.0595	+0.04	38.0589
C(7)	−0.04 [−0.06]	38.4613 [38.5134]	+0.03	38.0352	+0.02	38.0252

^aAtomic charges are given in e, atomic energy in au (absolute values). ^bThe values for the second independent molecule are given in brackets.

closely by quantum chemical calculations: $O\cdots H$ 2.382 Å, $\rho(r)$ 0.10 e Å^{−3}, $\nabla^2\rho(r)$ 1.4 e Å^{−5}, and E_{int} 3.4 kcal/mol.)

Note that these topological parameters for the chemical bonds in the anomeric unit O–N–O mirror the weakening of the bond N(1)–O(2) ($\rho(r) = 1.72$ e Å^{−3}, $\nabla^2\rho(r) = 8.9$ e Å^{−5}) as compared to N(1)–O(1) ($\rho(r) = 2.17$ e Å^{−3}, $\nabla^2\rho(r) = 5.2$ e Å^{−5}) observed in their lengths; the positive sign of the Laplacian at their BCPs indicate a certain depletion of the electron density, which is a well-known feature.^{15,35} Although displaying the same trend, the values $\rho(r)$ and $\nabla^2\rho(r)$ for the second independent molecule are slightly different: 1.74 vs 2.21 e Å^{−3} and 8.0 vs 4.9 e Å^{−5}. This variation can be accounted for the natural spread of $\rho(r)$ and $\nabla^2\rho(r)$ values, which were shown to vary by 0.1 e Å^{−3} and 3–4 e Å^{−5} for chemical bonds (see ref 36 and references therein) as well as for a slight variation in the N–O bond lengths. For comparison, the bonds O(1)–C(1) and O(2)–C(5) are characterized by $\rho(r)$ equal to 1.65 and 1.79 e Å^{−3} and $\nabla^2\rho(r)$ equal to −4.5 and −7.7 e Å^{−5}, respectively (1.65 e Å^{−3}, −5.5 e Å^{−5} vs 1.83 e Å^{−3}, −8.6 e Å^{−5} for the other molecule); all agreeing with their bond lengths.

Although the difference in these properties for the bonds N(1)–O(1) and N(1)–O(2) is in line with the hyperconjugative model of the SEI $\text{lp}(\text{O}1) \rightarrow \sigma^*(\text{N}1-\text{O}2)$,⁸ the atomic charges and energies within the second interpretation of SEIs give controversial results. Their values obtained experimentally (Table 2) demonstrate that the atom O(2) has a higher electronic population and energy (by the absolute value) than the atom O(1) (−0.63 e and −75.2202 au against −0.60 e and −75.1760 au). The same is observed for the second independent molecules (−0.63 e and −75.2526 au for O(2) against −0.59 e and −75.2173 au for O(1)), as if the charge and energy came from the atom O(1) to O(2) (and from O(1A) to O(2A)). The latter fact agrees with the theoretical finding that a SEI lp-X-C-Y occurs with a loss of charge and energy by the atom X and gain of it by the atom Y.^{13,14} Note that the carbon atoms adjacent to these oxygens in **1** bear the most positive charge +0.16 and +0.21 e (+0.19 and +0.23 e for the other molecule) for the atoms C(1) and C(5), respectively, with the largest value in the latter case. The atomic charges for the other atoms of the core vary from −0.29 to −0.04 e; the atom C(4) bearing slightly positive charge of +0.09 and +0.07 e.

The difference in the experimental energies (Table 2) of the two oxygen atoms O(1) and O(2) is 27.7 and 22.1 kcal/mol in the two independent species of **1**. The two values are rather

close, together with the individual and net atomic charges and energies (the differences in these values for the two molecules are 0.002 e and 0.01964 au) reflecting the pseudo-symmetric relation between the independent species. If we assume this difference to be the result of a transfer of energy from O(1) to O(2) accompanying the SEI $\text{lp-O}(1)-\text{N}(1)-\text{O}(2)$, it would be a nice quantitative estimate of its strength. However, in the absence of the hydrogens and their substitutes at the central atom, N(1) in this case, the other atoms may still be involved in the charge and energy processes within the anomeric unit. Those may include, e.g., the above SEIs $\text{lp-N}(1)-\text{O}(1)-\text{C}(1)$ and $\text{lp-N}(1)-\text{C}(3)-\text{C}(4)$ in **1**.

Quantum Chemical Calculation of **1 and Its Sister Isomer **1_noanomer**.** To find this out, we have performed the quantum chemical calculations of **1** and its sister isomer **1_noanomer** (i.e., with and without the SEI $\text{lp-O}(1)-\text{N}(1)-\text{O}(2)$); the latter is different from **2** in that it has exactly the same substituents at the heterocyclic core as the compound **1** does. In both cases, the molecular geometry (Table 1) was reproduced closely (in **1**, as the average of the two independent molecules) as well as the trend in the oxygens' charges and energies (Table 2; see also Table S2 of Supporting Information). In the isolated molecule **1**, their absolute values are also higher for the atom O(2) (−0.71 e and −75.6915 au against −0.64 e and −75.6409 au); those in **1_noanomer** are practically equal (−0.69 e and −75.7054 au against −0.69 e and −75.7090 au). Note that the experimental charges of the two oxygen atoms in **1** (−0.63 and −0.60 e for O(2) and O(1), respectively) are somewhat close to each other, which can be the result of the intermolecular interactions $\text{C-H}\cdots\text{O}$ with the atom O(1) (all together having nearly the same energy as the above intramolecular $\text{C}(2)-\text{H}(2\text{B})\cdots\text{O}(2)$ bond) affecting its charge in a crystal (see Supporting Information) or other SEIs in the molecule (see below).

The difference in the energy of the atoms O(1) and O(2) in the isolated **1** and **1_noanomer** is 31.8 and 2.2 kcal/mol, respectively; the former matches quite nicely the largest value obtained from the experimental electron density distribution (27.7 kcal/mol).

The difference in electron populations of these atoms in the two isomers is, however, not exactly as predicted by the hyperconjugative model of the SEI. Although the oxygen charges vary by the same magnitude but in different directions (O(1) loses 0.03 e, and O(2) accepts ~0.02 e), the most pronounced changes are observed for the atom C(1), which

acquires 0.07 e going from **1_noanomer** to **1**. At the same time, the evolution of the atomic energies reveals the largest variation in the case of O(1), with the atom C(1) being the second to it. These two are correspondingly the atoms that destabilize (O(1) by 0.0681 au) and stabilize (C(1) by 0.0393 au) the most among others, when going from **1_noanomer** to **1**. The latter also causes a significant increase in the atomic energy for the atom N(1) and its decrease for O(2), by 0.0238 and 0.0139 au. Overall, there is a clear destabilization of a whole ONO unit when involved in the SEI lp-O(1)–N(1)–O(2); in that case, its net atomic energy is 36.5 kcal/mol lower by the absolute value. If all the non-hydrogen atoms of the core are concerned, this value goes down to 7.4 kcal/mol, yet favoring **1_noanomer**. However, the energy difference between the two isomers is 0.02 kcal/mol in favor of one with the SEI lp-O(1)–N(1)–O(2).

Quantum Chemical Calculation of Model Systems. To get more insight into the role of this SEI in the absence of the steric effects, which apparently play a very important role in stabilizing the isomer **1**, we performed the similar analysis for the model systems **1_core** and **2_core** (Scheme 1) with the same core as in **1** and **2** but with no substituents (Figure 4).

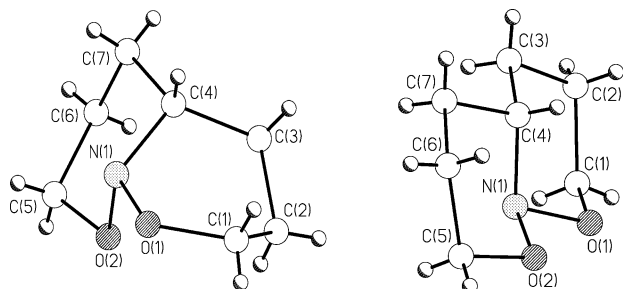


Figure 4. Model compounds having no substituents at the heterocyclic core with (**1_core**, left) and without (**2_core**, right) the SEI lp-O(1)–N(1)–O(2).

These are two isomers with and without the SEI lp-O(1)–N(1)–O(2), as judged by the N–O bond lengths (Table 3)

Table 3. Selected Bond Lengths in the Model Systems **1_core and **2_core** and Their Protonated Analogues (in Å)**

bond	1_core	2_core	1_coreH+	2_coreH+
N(1)–O(1)/N(1)–O(2)	1.388/1.476	1.436	1.379/1.423	1.401
O(1)–C(1)/O(2)–C(5)	1.457/1.426	1.427	1.483/1.464	1.467
C(1)–C(2)/C(5)–C(6)	1.518/1.531	1.529	1.513/1.521	1.519
C(2)–C(3)/C(6)–C(7)	1.539/1.538	1.535	1.542/1.537	1.534
C(3)–C(4)/C(4)–C(7)	1.549/1.540	1.535	1.540/1.536	1.530
N(1)–C(4)	1.483	1.484	1.528	1.526

and the NBO data. The evolution of the bond lengths upon going from one to the other (similar to that for the parent compounds **1** and **2**) exhibits lengthening/shortening trends expected from the charge transfer considerations of SEI lp(X) $\rightarrow \sigma^*(Z-Y)$ involving N–O and other bonds (Table S4 of Supporting Information).

The most pronounced changes are observed for the bonds N(1)–O(1) and N(1)–O(2) that vary by 0.04–0.05 Å going

from **2_core** to **1_core**. This agrees with the NBO analysis showing the presence of the strong SEI lp(O1) $\rightarrow \sigma^*(N1-O2)$ in **1_core** with the energy of 16.34 kcal/mol. A very similar value was obtained for the compound **1** (16.09 kcal/mol).

Those for additional SEIs according to the NBO results (their total energy for both forms being close) explain other discrepancies in the bond lengths. In particular, the second and the third strongest SEIs (8.23–8.93 and 6.28–6.58 kcal/mol), which are present in **1** and **1_core** only, are lp(N1) $\rightarrow \sigma^*(O1-C1)$ and lp(N1) $\rightarrow \sigma^*(C3-C4)$. The latter is in line with the observed lengthening of the bonds O(1)–C(1) and C(3)–C(4) (by ~ 0.03 and ~ 0.01 Å, respectively) upon going from the molecules with the above SEI lp-O(1)–N(1)–O(2) to those that lack it.

To eliminate the contribution from the above two strong SEIs formally involving the lone pair of the nitrogen atom (and to be able to relate the difference in the oxygen atomic energy with the strength of the SEI lp-O(1)–N(1)–O(2)), we have also carried out the quantum chemical calculations of the protonated analogues of **1_core** and **2_core**. According to its results, the asymmetry of the ONO unit in the former persists (1.379 vs 1.423 Å), and the strongest SEI here is lp-O(1)–N(1)–O(2) with the NBO energy of 14.88 kcal/mol; for others, it is not higher than 5.5 kcal/mol (see Table S5 of Supporting Information).

Despite this, no anomeric stabilization of **1_core** or its protonated analogue is observed; the total energy of the symmetric isomer is lower by 5.2 and 3.2 kcal/mol for the neutral and protonated forms, respectively. The latter, however, agrees with the fact that among the above 71 compounds from CSD (version 5.33, 2011) only one has two 6-membered rings fused through the ONO fragment (refcode NIOXIS); this is a derivative of the model systems with the NO₂ group at the C(4) atom and two nearly identical N–O bonds. Note that a new series of related compounds with CCDC 912759–912762 (see above) also displayed the preference for a symmetric conformation that lacks the SEI in the ONO unit, and the stabilization of **1** as a distorted isomer is apparently achieved not by the SEI lp-O(1)–N(1)–O(2) but through introducing some substituents [compare with **1_core**].

AIM-based atomic energies for the ONO unit also reveal the nonstabilizing character of this SEI. In neutral **core** molecules, it causes a significant destabilization of the atom O(1) by 0.0386 au and a small one of O(2) (by 0.0078 au), which is not compensated for by the change in the nitrogen's atomic energy increasing by 0.0083 au. As a result, the ONO unit loses 23.9 kcal/mol when placed in the distorted isomer **1_core** with the SEI lp-O(1)–N(1)–O(2), which according to NBO data has a high stabilization energy. This, however, agrees with the recent finding that a hyperconjugation may play a negative role in the conformational preferences of a series of acyclic molecules.⁶

In the protonated species, the same SEI lp-O(1)–N(1)–O(2) in the distorted isomer is weaker (with the NBO energy of 14.88 kcal/mol), the delocalization through the NH group is less efficient, so its destabilization effect is lower and thus the net atomic energy for the unit ONO is more favorable in **1_coreH+** than in **2_coreH+** (by 1.3 kcal/mol), although in overall the latter is still more stable than the former. If, however, the hydrogen atom at N(1) is taken into account, the whole ON(H)O moiety destabilizes by 4.4 kcal/mol following the total energies of the two isomers. The destabilizing character of such a strongly stabilizing interaction according to NBO (~ 15 – 16 kcal/mol) is, apparently, not a unique

Table 4. Atomic Charges and Energies^a Calculated for the Core Atoms in 1_core and 2_core and Their Protonated Analogues

atom	1_core		2_core		1_coreH+		2_coreH+	
	charge	energy	charge	energy	charge	energy	charge	energy
N(1)	−0.04	54.7062	−0.06	54.7140	−0.06	54.7883	−0.06	54.7905
O(1)	−0.65	75.6507	−0.68	75.6893	−0.57	75.6270	−0.56	75.6358
O(2)	−0.72	75.6975	−0.68	75.6893	−0.60	75.6488	−0.56	75.6358
C(1)	+0.43	37.8088	+0.48	37.7700	+0.36	37.8453	+0.38	37.8339
C(2)	+0.05	38.0240	+0.04	38.0245	+0.05	38.0280	+0.05	38.0285
C(3)	+0.04	38.0153	+0.04	38.0210	+0.04	38.0281	+0.03	38.0293
C(4)	+0.31	37.8989	+0.30	37.9232	+0.22	37.9357	+0.23	37.9537
C(5)	+0.48	37.7677	+0.48	37.7700	+0.38	37.8315	+0.38	37.8339
C(6)	+0.04	38.0233	+0.04	38.0245	+0.04	38.0278	+0.05	38.0285
C(7)	+0.05	38.0143	+0.04	38.0210	+0.03	38.0245	+0.03	38.0293

^aAtomic charges are given in e, atomic energy in au (absolute values).

feature of the unit ONO; it was also found to be the case of the same model systems but with CH group instead of NH. Although not reproducing the exact trends in the atomic energies (see Supporting Information), the quantum chemical calculations of the latter show that the total energies as well as those of a OCO or a OC(H)O unit favor the isomer without the SEI lp-O(1)–C(X)–O(2) by 4.0, 9.1, and 11.2 kcal/mol, respectively, and the atom that destabilizes the most (by 0.0270 kcal/mol) is C(4).

In the case of 1_coreH+, this is also the atom C(4) (by 0.0181 au), with the atom O(1) being second to it (0.0078 au). The similar destabilization of the atom C(4), although even more pronounced (by 0.0243 au), is observed for the neutral species. Note that the changes in the C(4) atomic energy going from the parent compound 1 to 1_noanomer, which are also among the largest, are of the same order of magnitude (0.0133 au) but favor the isomer with the SEI lp-O(1)–N(1)–O(2). This, to some extent, offsets the huge destabilization originated from the atom O(1) therein.

Nevertheless, the changes in atomic charges and energies (Tables 4 and S3 of Supporting Information) upon the formation of the SEI lp-O(1)–N(1)–O(2) in both the neutral and protonated core species agree with the standard scheme: the transfer of charge (0.035 and 0.030 e, respectively) to the atom O(2). This is also accompanied by a large gain (of 0.052 and 0.014 e) of electron population by the atom C(1) similar to one observed between 1 and 1_noanomer (0.066 e). The corresponding difference in its atomic energy also matches that for the substituted compounds (0.0387 au between the neutral and 0.0114 au between the protonated isomers against 0.0393 au between 1 and 1_noanomer). For comparison, the same values for the hydrogen atoms do not exceed 0.029 e and 0.0112 au (0.046 e and 0.0177 au in the case of the substituted compounds).

Note that the atomic energies for the atoms O(2) and N(1) in 1_core and 2_core varies little, by 0.0083 and 0.0078 au, so the difference in oxygen energies can be a direct estimate of their perturbation as a result of the SEI lp-O(1)–N(1)–O(2). There is even a very good quantitative agreement between the values of the atomic energy differences between O(1) and O(2): 27.7 kcal/mol from the experimental data for 1; 31.8 and 29.4 kcal/mol from the quantum chemical calculations of the substituted and unsubstituted molecules. Note that the same differences of 28.3 (22.1 kcal/mol for the second independent molecule), 31.2, and 25.8 kcal/mol, respectively, are observed between the atoms C(1) and C(5) bound to these oxygen atoms. The values thus obtained are two times larger than the

stabilization energy through the charge delocalization lp(O1) → $\sigma^*(\text{N1}–\text{O2})$ from the NBO analysis (~16 kcal/mol). For comparison, the atomic energies of sulfur atoms¹³ vary by 17.8 kcal/mol as a result of weaker stereoelectronic interaction lp–N–C–S, as evidenced by the smaller difference in the C–S bond lengths (0.046 Å) compared to the N–O ones (0.079 Å in a crystal) and the NBO energy of 9.3 kcal/mol.

If, however, the protonated forms of 1_core and 2_core are concerned, the largest variations of the atomic energies within the ONO unit by 0.0130 au is observed for the atom O(2), while those for O(1) and N(1) are much lower (0.0088 and 0.0020 au). In this case, with the contribution from other SEIs largely minimized, the difference between the two oxygens is equal to 13.7 kcal/mol, which is surprisingly close to the energy of the SEI lp-O(1)–N(1)–O(2) estimated by the NBO analysis to be 14.9 kcal/mol. Although there is only a semiquantitative agreement between the energy values obtained by the AIM analysis and calculated from the NBO data for the above neutral systems, they clearly reflect the degree of perturbation of a system by the SEI. So the atomic energies that can be thus obtained in one pot even from the experimental data provide another measure of its strength than NBO that takes into account its destabilizing character and the presence of other (competitive or cooperative) SEIs.

CONCLUSIONS

The examination of the electron density distribution for [1,2]oxazino[2,3-b][1,2]oxazine derivatives with the ONO unit having a geometry formally governed by the stereoelectronic interaction lp-O(1)–N(1)–O(2) and their isomers without it allowed investigating the variations of atomic charges and energies because of it. This interaction results in a clear loss of energy by the oxygen atom that acts as a donor of a lone pair according to the hyperconjugative model, while that for the nitrogen and the second oxygen atom remains relatively constant; so their difference was used for the first time as a measure of a SEI obtained solely from the experimental data. The AIM-based atomic energies within the ONO unit, both calculated and obtained experimentally, provided the estimates for the strength of the SEI lp-O(1)–N(1)–O(2) that were consistent with the NBO data; when other SEIs were blocked, the agreement was even quantitative. With these two methods (one being very sensitive to other SEIs and one lacking the possibility of judging to which extent a SEI should be strong to be significant), such a consistency may be expected for a strong stereoelectronic interaction in other systems, although in the case of weak SEIs, it may be rather random in nature.

Table 5. Differences in the Total Energies^a of the Isolated Isomers among the Systems (Molecules or Cations) Studied, Those in the AIM-Based Net Energies of the ONO Unit^b and the NBO Energies of the SEI lp-O(1)–N(1)–O(2) Where Present (All Values Are Given in kcal/mol)

parameter	1 – 1_noanomer	1_core – 2_core	1_coreH+ – 2_coreH+
ΔE_{mol}	–0.02	5.2	3.2 (4.0) ^c
ΔE_{ONO}	36.5	23.9	4.4 (11.2)
E_{NBO}	16.09	16.34	14.88 (16.1)

^aValues with ZPE taken into account. ^b ΔE_{ONO} for the protonated species was calculated with hydrogen atom taken into account. ^cThe values in the parentheses are given for the carbon-containing analogues of the protonated core species.

However, AIM-based atomic energies (Table 5) also allowed revealing the destabilizing character of the SEI lp-O(1)–N(1)–O(2), in contrast to the NBO analysis that indicated it to be stabilizing, as SEIs are usually believed to be. This, together with the results reported recently for a series of acyclic molecules,⁶ clearly shows that the role SEIs play in conformational preferences should be scrutinized on a systematic basis, and the AIM-based approach is a very convenient tool to deal with it.

■ ASSOCIATED CONTENT

● Supporting Information

Supplementary figures and tables mentioned in the text as well as the outputs of the multipole refinement for **1**. This material is available free of charge via the Internet at <http://pubs.acs.org>.

■ AUTHOR INFORMATION

Corresponding Author

*E-mail: unelya@xrlab.ineos.ac.ru (Y.V.N.).

Author Contributions

The manuscript was written through contributions of all authors. All authors have given approval to the final version of the manuscript.

Notes

The authors declare no competing financial interest.

■ ACKNOWLEDGMENTS

We would like to thank A. A. Tabolin and E. O. Gorbacheva (Institute of Organic Chemistry of Russian Academy of Sciences, Moscow, Russia) for providing the crystals of the compounds **1** and **2**. This paper is dedicated to Professor S. M. Aldoshin on the occasion of his 60th birthday. This study was financially supported by the Russian Foundation for Basic Research (Projects 12-03-33107 and 13-03-00772) and the Foundation of the President of the Russian Federation (Grants MK-6938.2012.3 and MD-1020.2012.3).

■ REFERENCES

- (1) Kirby, J. *The Anomeric Effect and Related Stereoelectronic Effects at Oxygen*; Springer Verlag: New York, 1983.
- (2) Deslongchamps, P. *Stereoelectronic Effects in Organic Chemistry*; Wiley: New York, 1983.
- (3) Brunk, T. K.; Weinhold, F. Quantum-Mechanical Studies on the Origin of Barriers to Internal Rotation about Single Bonds. *J. Am. Chem. Soc.* **1978**, *101*, 1700–1709.
- (4) Salzner, U.; Schleyer, P. V. Generalized Anomeric Effects and Hyperconjugation in $\text{CH}_2(\text{OH})_2$, $\text{CH}_2(\text{SH})_2$, $\text{CH}_2(\text{SEH})_2$, and $\text{CH}_2(\text{TEH})_2$. *J. Am. Chem. Soc.* **1993**, *115*, 10231–10236.
- (5) Salzner, U.; Schleyer, P. V. Ab-initio Examination of Anomeric Effects in Tetrahydropyrans, 1,3-Dioxanes, and Glucose. *J. Org. Chem.* **1994**, *59*, 2138–2155.

(6) Wang, C.; Chen, Z.; Wu, W.; Mo, Y. How the Generalized Anomeric Effect Influences the Conformational Preference. *Chem.—Eur. J.* **2012**, *19*, 1436–1444.

(7) Shishkina, S. V.; Slabko, A. I.; Shishkin, O. V. Conjugation vs Hyperconjugation in Molecular Structure of Acrolein. *Chem. Phys. Lett.* **2013**, *556*, 18–22.

(8) Vila, A.; Mosquera, R. A. Atoms in Molecules Interpretation of the Anomeric Effect in the O–C–O Unit. *J. Comput. Chem.* **2007**, *28*, 1516–1530.

(9) Vila, A.; Mosquera, R. A. QTAIM Explanation of the Anomeric Effect in the O–C–O Unit II: 2-Methoxyoxane and 2,2-Dimethoxypropane. *Chem. Phys. Lett.* **2007**, *443*, 22–28.

(10) Eskandari, K.; Vila, A.; Mosquera, R. A. Interpretation of Anomeric Effect in the N–C–N Unit with the Quantum Theory of Atoms in Molecules. *J. Phys. Chem. A* **2007**, *111*, 8491–8499.

(11) Bader, R. F. W. *Atoms in Molecules. A Quantum Theory*; Clarendon Press: Oxford, U.K., 1990.

(12) Bushmarinov, I. S.; Lyssenko, K. A.; Antipin, M. Y. Atomic Energy in the ‘Atoms in Molecules’ Theory and Its Use for Solving Chemical Problems. *Russ. Chem. Rev.* **2009**, *78*, 283–302.

(13) Bushmarinov, I. S.; Antipin, M. Y.; Akhmetova, V. R.; Nadyrgulova, G. R.; Lyssenko, K. A. Stereoelectronic Effects in N–C–S and N–N–C Systems: Experimental and Ab-initio AIM Study. *J. Phys. Chem. A* **2008**, *112*, 5017–5023.

(14) Bushmarinov, I. S.; Antipin, M. Y.; Akhmetova, V. R.; Nadyrgulova, G. R.; Lyssenko, K. A. The lp-S-C-NH+ Stereoelectronic Interaction and Effect of Hydrogen Bonding on it. *Mendeleev Commun.* **2009**, *19*, 14–16.

(15) Nelyubina, Y. V.; Antipin, M. Y.; Cherepanov, I. A.; Lyssenko, K. A. Pseudosymmetry As Viewed Using Charge Density Analysis. *CrystEngComm* **2010**, *12*, 77–81.

(16) Nelyubina, Y. V.; Daling, I. L.; Lyssenko, K. A. Pseudosymmetry in Trinitroprazole: The Cost of Error in Space-Group Determination. *Angew. Chem., Int. Ed.* **2011**, *50*, 2892–2894.

(17) Sheldrick, G. M. A Short History of SHELX. *Acta Crystallogr., Sect. A: Found. Crystallogr.* **2008**, *64*, 112–122.

(18) Hansen, N. K.; Coppens, P. Electron Population Analysis of Accurate Diffraction Data 0.6. Testing Aspherical Atom Refinements on Small-Molecule Data Sets. *Acta Crystallogr., Sect. A: Found. Crystallogr.* **1978**, *34*, 909–921.

(19) Volkov, A.; Macchi, P.; Farrugia, L. J.; Gatti, C.; Mallinson, P.; Richter, T.; Koritsanszky, T. XD2006, a Computer Program for Multipole Refinement, Topological Analysis of Charge Densities and Evaluation of Intermolecular Energies from Experimental or Theoretical Structure Factors; SUNY at Buffalo: Buffalo, NY, 2006.

(20) Su, Z. W.; Coppens, P. On the Calculation of the Lattice Energy of Ionic-Crystals Using the Detailed Electron-Density Distribution 0.1. Treatment of Spherical Atomic Distributions and Application to NaF. *Acta Crystallogr., Sect. A: Found. Crystallogr.* **1995**, *51*, 27–32.

(21) Hirshfeld, F. L. Can X-Ray Data Distinguish Bonding Effects from Vibrational Smearing. *Acta Crystallogr., Sect. A: Found. Crystallogr.* **1976**, *32*, 239–244.

(22) Kirzhnits, D. A. Quantum Corrections to the Thomas-Fermi Approximation. *Sov. Phys. JETP* **1957**, *5*, 54.

(23) Stash, A.; Tsirelson, V. WinXPRO: a Program for Calculating Crystal and Molecular Properties Using Multipole Parameters of the Electron Density. *J. Appl. Crystallogr.* **2002**, *35*, 371–373.

- (24) Espinosa, E.; Molins, E.; Lecomte, C. Hydrogen Bond Strengths Revealed by Topological Analyses of Experimentally Observed Electron Densities. *Chem. Phys. Lett.* **1998**, *285*, 170–173.
- (25) Espinosa, E.; Alkorta, I.; Rozas, I.; Elguero, J.; Molins, E. About the Evaluation of the Local Kinetic, Potential and Total Energy Densities in Closed-Shell Interactions. *Chem. Phys. Lett.* **2001**, *336*, 457–461.
- (26) Nelyubina, Y. V.; Glukhov, I. V.; Antipin, M. Y.; Lyssenko, K. A. Higher Density Does Not Mean Higher Stability Mystery of Paracetamol Finally Unraveled. *Chem. Commun.* **2010**, *46*, 3469–3471.
- (27) Lyssenko, K. A.; Korlyukov, A. A.; Antipin, M. Y. The Role of Intermolecular H···H and C···H Interactions in the Ordering of [2.2]Paracyclophane at 100 K: Estimation of the Sublimation Energy from the Experimental Electron Density Function. *Mendeleev Commun.* **2005**, 90–92.
- (28) Sobczyk, L.; Grabowski, S. J.; Krygowski, T. M. Interrelation Between H-bond and Pi-Electron Delocalization. *Chem. Rev.* **2005**, *105*, 3513–3560.
- (29) Lyssenko, K. A. Analysis of Supramolecular Architectures: Beyond Molecular Packing Diagrams. *Mendeleev Commun.* **2012**, *22*, 1–7.
- (30) Frisch, M. J.; Trucks, G. W.; Schlegel, H. B.; Scuseria, G. E.; Robb, M. A.; Cheeseman, J. R.; Scalmani, G.; Barone, V.; Mennucci, B.; Petersson, G. A.; et al. *Gaussian 09*, revision A.1; Gaussian, Inc.: Wallingford, CT, 2009.
- (31) Keith, T. A. *AIMAll*, version 10.12.13; TK Gristmill Software: Overland Park KS, 2010; see <http://aim.tkgristmill.com>.
- (32) Cambridge Crystallographic Database (version 5.33), 2011.
- (33) Gorbacheva, E. O.; Tabolin, A. A.; Novikov, R. A.; Khomutova, Yu. A.; Nelyubina, Yu. V.; Tomilov, Yu. V.; Ioffe, S. L. Six-Membered Cyclic Nitronates as 1,3-Dipoles in Formal [3 + 3]-Cycloaddition with Donor–Acceptor Cyclopropanes. Synthesis of New Type of Bicyclic Nitrosoacetals. *Org. Lett.* **2013**, *15*, 350–353.
- (34) Savin, A.; Nesper, R.; Wengert, S.; Fassler, T. F. ELF: The Electron Localization Function. *Angew. Chem., Int. Ed.* **1997**, *36*, 1809–1832.
- (35) Lyssenko, K. A.; Antipin, M. Y.; Khrustalev, V. N. The Nature of the O–O Bond in Hydroperoxides. *Russ. Chem. Bull.* **2001**, *50*, 1539–1549.
- (36) Checinska, L.; Mebs, S.; Hubschle, C. B.; Forster, D.; Morgenroth, W.; Luger, P. Reproducibility and Transferability of Topological Data: Experimental Charge Density Study of Two Modifications of L-Alanyl-L-tyrosyl-L-alanine. *Org. Biomol. Chem.* **2006**, *4*, 3242–3251.